Article

Effects of changes in non-photosynthetic vegetation cover and grazing amount on rainfall erosion in grasslands on the Qinghai-Tibet Plateau

Xuhui Ding [1,2,*], Pengwei Chen [3], Huiqi Song [4], Mo Chen [1], and Muhammad Imran [1]

[1] School of Finance and Economics, Jiangsu University, Zhenjiang 212013, China; 2112219002@stmail.ujs.edu.cn (M.C.); imranecon@hotmail.com (M.I.)

[2] School of Finance and Economics, Qinghai University, Xining 810016, China

[3] Academy of Animal Husbandry and Veterinary Sciences, Qinghai University, Xining 810016, China; chenpengweixuexi@163.com

[4] School of Agricultural Economics and Rural Development, Renmin University of China, Beijing 100872, China; songhuiqi2020@163.com

Correspondence: dingxh@ujs.edu.cn

Graphical abstract

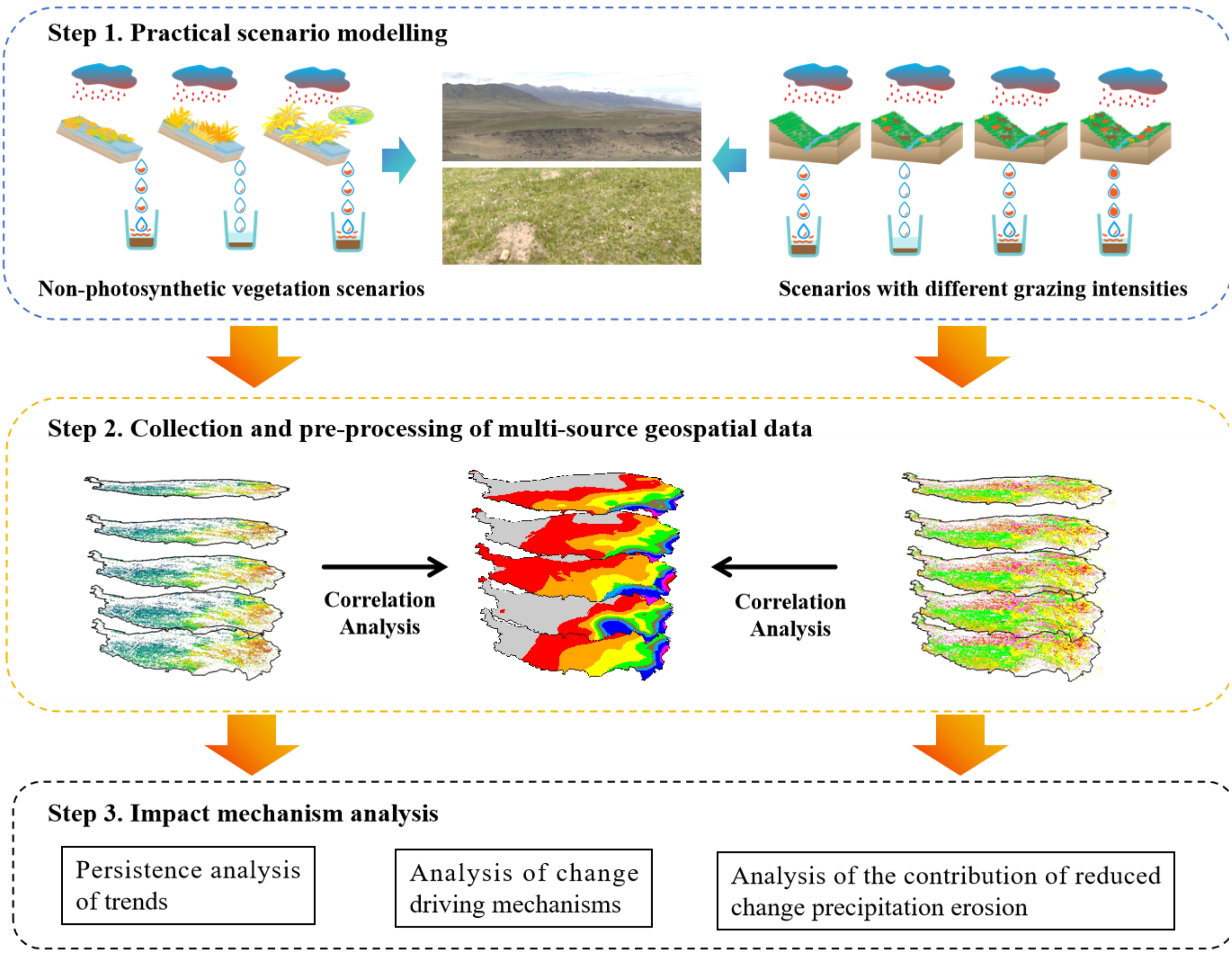

Abstract: Rainfall erosion is a complex environmental problem involving multiple influences, both natural and human. To explore effective strategies to suppress the erosive power of rainfall on the Qinghai-Tibet Plateau, researchers considered the complexity of regional geographic features. This paper also accounted for the variability of livestock carrying capacity across different grasslands. Based on the raster data of changes in non-photosynthetic vegetation cover and livestock carrying capacity on the Qinghai-Tibet Plateau from 2000 to 2019, this study employs partial correlation analysis and multiple residual regression. These methods are used to verify the correlation between precipitation erosive power and changes in non-photosynthetic vegetation cover. Additionally, the study assesses the contribution of these changes from the image metric perspective. The results showed that: (1) the erosive power of rainfall on the Qinghai-Tibet Plateau has experienced 'N'-shaped fluctuations, and its spatial distribution shows an increasing trend from northwest to southeast. (2) Non-photosynthetic vegetation cover was positively correlated with rainfall erosivity in the central part of the Plateau. However, it was negatively correlated in the southern and northeastern parts. The positive and negative correlation zones of grassland carrying capacity were staggered. (3) Non-photosynthetic vegetation cover and grassland livestock carrying capacity together affected 17.66% of the image area with increased rainfall erosivity. In contrast, only 3.07% of the image area experienced reduced rainfall erosivity. This imbalance raises the risk of overall rainfall erosivity. (4) The contribution of livestock carrying capacity to the increase of rainfall erosivity was 26.99%, which is higher than the 17.38% contribution of non-photosynthetic vegetation cover. Non-photosynthetic vegetation cover, however, played a more significant role in reducing rainfall erosivity. In order to provide a scientific basis for the land conservation and sustainable development of the Qinghai-Tibet Plateau, this study aims to offer valuable insights and recommendations.

Keywords: Rainfall erosivity; Qinghai-Tibetan Plateau; Combined contribution; Livestock carrying capacity; Pixel-wise Multivariate Analysis

1. Introduction

Rainfall erosion is a direct cause of land degradation and an environmental problem faced globally (Chen et al., 2022). The most fundamental source of power affecting soil erosion is rainfall. Influencing the erosive power of rainfall is a complex process caused by a combination of anthropogenic and natural factors (Lobo et al., 2018). Soil erosion accounts for an annual global loss of 75 billion tonnes of soil globally each year. Severe soil erosion leads to reduced land productivity and land degradation. Soil erosion causes economic losses of tens of billions of euros annually in the EU. It also poses a major threat to global food security and the Sustainable Development Goals (SDGs), impacting the well-being of at least 3.2 billion people worldwide. Therefore, effectively combating soil erosion by rainfall and building a better, more sustainable ecological environment has become an important and urgent task for governments globally.

Scholars agree that rainfall erosion causes significant problems, acting as a major driver of hydraulic erosion by moving soil particles. Investigating the factors affecting these changes can provide a basis for improving soil and water conservation and economic development in the region (Das et al., 2023). While excellent studies have explored the relationship between rainfall and soil, few have examined how precipitation erosion interacts with external factors (Johannsen et al., 2020). Some scholars noted that natural vegetation changes, variations in rainfall frequency due to climate change, and human disturbances directly impact rainfall's erosive power (He et al., 2022; Panagos et al., 2015; Yan et al., 2023). Luciano et al. (2009) took a microscopic view, highlighting that vegetation cover is crucial in mitigating rainfall erosion. Additionally, it has been suggested that uncontrolled human activity demands are at the root of increased rainfall erosion (Busnelli et al., 2006). Soil and water conservation on the Tibetan Plateau, characterized by unique natural geography and climatic conditions, remains a serious challenge (Chen, Duan, Ding, et al., 2022). Few studies have analyzed the factors influencing rainfall erosion's erosive power there. Given this context, understanding natural elements and human economic activities can help identify key strategies for reducing precipitation erosion.

2. Literature review

The erosive power of rainfall has been a hot topic of research and concern for scholars, particularly in representative areas(Petek et al., 2018). For example, Johannsen et al. (2020) studied the transition from a temperate oceanic climate to a temperate continental climate in Austria. They evaluated the rainfall erosivity using rainfall data from 1995 to 2015 from meteorological stations across the country. By revealing the changes in the spatial and temporal distribution of rainfall erosive power, they reflected the potential soil erosion risk (Lisbeth L Johannsen et al., 2022). Studies on the impacts of rainfall erosivity on watersheds have focused on the temporal and spatial characteristics of the study area. These studies often divide the area into the upper, middle, and lower reaches, or base the division on administrative boundaries (Chang et al., 2022). However, this approach may not fully capture the variability of rainfall erosivity within the region. Related studies for the plateau region focus more on estimation models, quantification, spatial and temporal distribution patterns of rainfall erosivity, and their evolutionary trends (Fan et al., 2013; Lu et al., 2023). For example, rainfall erosion rates for the Loess Plateau of China from 1981 to 2020 were calculated based on the GEE platform (Zeng et al., 2023). Based on rainfall data from the Qinghai-Tibet Plateau between 1991 and 2020, Liu et al. analyzed the distribution of annual precipitation erosive forces in the region in detail (Liu et al., 2022). As a result, numerous studies have focused on exploring the temporal and spatial distribution characteristics of rainfall erosive power and its evolution. However, these studies have neglected the investigation of the drivers of rainfall erosive power in geographically distinctive regions (He et al., 2018).

The increase in vegetation cover can effectively reduce the impact of rainfall on the soil. It also reduces soil erosion caused by runoff and helps improve soil structure. These factors are important in mitigating soil erosion .In their five-year-long experiment, Li et al. found that citrus tree plantings were present in the plots (Li et al., 2014). However, Bahia grass (Paspalum notatum Flugge) mulch was still necessary for soil retention. Erosive precipitation affects vegetation cover, which in turn influences surface erosion processes. Monitoring and evaluating of changes in regional vegetation cover is necessary. This is essential to capture regional soil erosion risks (Souza et al., 2018). There is a relationship between rainfall erosivity and geographic and anthropogenic factors (Abd Aziz et al., 2012; Angulo-Martínez et al., 2012). Khanal et al. (2013) noted regional changes in rainfall erosion and soil erosion due to land use and land cover changes induced by biofuel policies.

Cogo et al. (2003)pointed out that increasing the above-ground biomass of crops leads to a significant increase in the amount of crop residue. This, in turn, increases the percentage of soil cover and reduces soil erosion caused by rainfall. Non-photosynthetic vegetation includes withered surface vegetation and dead branches and stems after plant decay (Li et al., 2018). This type of vegetation plays a crucial role in controlling wind and water erosion (Vrieling et al., 2014). Alves et al., (1995) noted that crop residue management had the lowest impact on soil erosion and runoff rates in no-tillage. Many studies have explored how vegetation cover reduces rainfall erosivity. However, research on non-photosynthetic vegetation cover is limited and has primarily focused on plantations.

The faecal emissions produced by livestock have a dual effect on plants. Moderate amounts of manure can benefit plant growth and help increase non-photosynthetic vegetation cover (Feng et al., 2023; Jiang et al., 2022). Reductions in grazing pressure and changes in seasonal grazing patterns may affect grassland yield trends. These changes can indirectly influence soil loss (Fan et al., 2010). The Qinghai-Tibet Plateau experiences diminished soil conservation services due to increased rainfall, which simultaneously alleviates grassland-livestock conflicts. However, rainfall erosion also enhances rhizosphere soils that cannot be restored within a short period. (Huang et al., 2018). Using the G2 model in Crete, Panagos et al. (2014) found elevated annual erosion data for natural grasslands and scrub. This was attributed to the intensification of livestock husbandry in recent decades. The Food and Agriculture Organization of the United Nations (FAO) has pointed out that overgrazing significantly increases and accelerates soil erosion. The land erosion rate under intensive grazing is 100 to 1000 times higher than the natural erosion rate. Currently, studies on the evolution trends of rainfall erosive force in the Qinghai-Tibet Plateau and its geographical distribution characteristics have achieved substantial results. However, the interaction between grassland non-photosynthetic vegetation cover and the changes in livestock carrying capacity and rainfall erosion in this region still needs to be deeply investigated (Cui et al., 2021). As a result, most studies have focused on single factors, such as small-scale crop residues and grazing. However, there is still a gap in the study of rainfall erosivity in its natural state, particularly in large-scale areas and in non-green vegetation cover in different geographic environments.

The Tibetan Plateau is an ecologically fragile area subject to significant anthropogenic disturbances. Over the past few decades, abnormal non-photosynthetic vegetation cover and increased annual precipitation have led to extensive grassland being affected by rainfall erosion. This poses a constant threat to livestock production on the Tibetan Plateau and has had serious impacts on the ecosystem and socio-economic development (Shen et al., 2024). As the effects of climate change are studied in greater depth, clarifying the indirect impacts of climate change and its relationship with the plateau ecosystem has become increasingly important. Since the mid-20th century, the Tibetan Plateau has experienced land degradation and desertification due to various anthropogenic factors, including overgrazing and mineral resource exploitation (Dong et al., 2020). Additionally, secondary hazards such as livestock waste have exacerbated these issues (Jiang et al., 2023). Slope is a critical factor contributing to soil erosion, and the unique topography and geomorphology of the Tibetan Plateau make it particularly vulnerable to this phenomenon. The indirect impacts of climate change and human activities on the plateau have become a focal point of academic research and an urgent issue requiring practical solutions.

Based on the shortcomings and real-world problems identified in previous studies, this study aims to quantify the effects of non-photosynthetic vegetation cover and grassland carrying capacity on the changes in rainfall erosivity on the Qinghai-Tibet Plateau. Long-term time series data, trend analysis, partial correlation analysis, and residual trend analysis were employed to elucidate the spatial and temporal evolution characteristics of rainfall erosivity at different temporal and spatial scales on the Qinghai-Tibet Plateau from 2000 to 2019. The study explores the impacts of non-photosynthetic vegetation cover and grassland carrying capacity on the variations in rainfall erosivity at different stages. It also proposes the differences in the impacts of non-photosynthetic vegetation cover and grassland carrying capacity on rainfall erosivity. Additionally, the study suggests the differences in the effects of non-photosynthetic vegetation cover and the amount of livestock in grasslands on rainfall erosivity. The marginal contributions of this study include: (1) analysing the spatial and temporal variability of rainfall erosivity on the Qinghai-Tibet Plateau at a large scale. (2) evaluates the correlation between non-photosynthetic vegetation cover and livestock carrying capacity with rainfall erosivity. (3) To investigate the driving mechanism of rainfall erosivity under both independent and coupled conditions of non-photosynthetic vegetation cover and livestock carrying capacity. (4) To clarify the contribution of non-photosynthetic vegetation cover and livestock carrying capacity in suppressing rainfall erosion both independently and in a coupled state. This study may provide a valuable reference for mitigating rainfall erosion and promoting sustainable soil development in highland regions globally.

3. Methods and Data

3.1. Study Area

The Qinghai-Tibet Plateau, located at (26°00′~39°47′N,73°19′~104°47′E) in central Asia, is the largest and highest plateau on Earth, known as the 'Roof of the World'. It covers a total area of about 2.5 million square kilometres (Figure 1). The region includes a series of high mountain ranges, such as the Himalayas, the Kunlun Mountains, and the Tanggula Mountains, and is dotted with numerous lakes and river headwaters. The climate is characterized by a highland or cold arid climate, with an average annual precipitation of around 400 mm. However, in the context of global warming, precipitation on the Qinghai-Tibet Plateau has shown an upward trend. From 1961 to 2020, annual precipitation increased by an average of about 7.9 mm per decade. In the central regions, such as the Sanjiangyuan, this value has increased by 5 to 20 mm per decade. The increase in precipitation has made areas lacking protection from non-photosynthetic vegetation more prone to severe rainfall erosion, exacerbating the problem of soil degradation. Despite this, the Qinghai-Tibet Plateau remains one of the more livestock-carrying regions of China. Due to its unique geographical location and extreme diversity of geomorphological features, as well as its fragile ecological environment, the Qinghai-Tibet Plateau has become an significant hotspot for scientific research around the world.

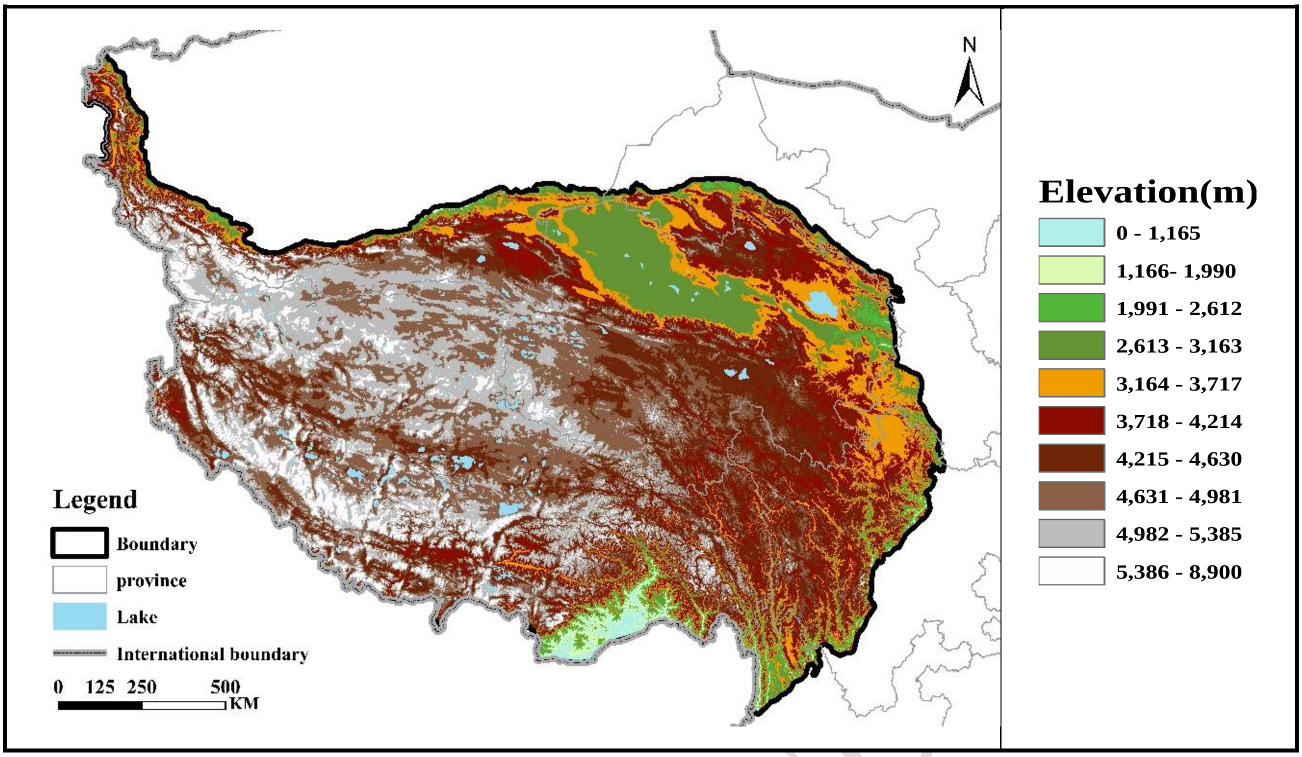

Figure 1 DEM 500 m on the Qinghai-Tibetan Plateau

3.2 Methods

1) Trend analysis

Linear regression is widely used to analyse spatial trends in the Earth's systems (Gao et al., 2017). The slope (L) of the rainfall erosive force from remote sensing images was fitted image by image to obtain the spatial trend of rainfall erosive force over n years. This was calculated as follows:

$$\boldsymbol{L}=\frac{n\times\sum_{i=1}^{n} i\times N_i-\sum_{i=1}^{n} i\times\sum_{i=1}^{n} N_i}{n\times\sum_{i=1}^{n} i^2-\left(\sum_{i=1}^{n} i\right)^2} \quad (1)$$

Where: L_i is the average annual rainfall erosive power in year ii; n is the length of the study period, with n = 20. Significance was tested using the F-test. The formulae are given below:

$$\boldsymbol{F}=\frac{\sum_{i=1}^{n}(\hat{y}_i-\bar{y})^2}{\Sigma(y_i-\hat{y}_i)^2/(n-2)} \quad (2)$$

Where: $\hat{y}_i$ is the linear regression value of rainfall erosivity in year *i*; y_i is the rainfall erosivity in year *i*; n-2 is the residual degree of freedom.

The magnitude of change in rainfall erosion (Q) represents the direction of change in rainfall erosion over time. When Q > 0, it indicates that rainfall erosion is increasing, and the larger the value, the faster the increase. Conversely, when Q < 0, it indicates that rainfall erosion is decreasing. The calculation formula is as follows:

$$\boldsymbol{Q} = S(n-1) \quad (3)$$

2) Hurst Index

The Hurst index is an effective method for quantitatively describing the long-term dependence of a time series. The calculation formula is as follows:

$$\overline{\boldsymbol{N}(\boldsymbol{t})} = \frac{1}{t}\Sigma_{i=1}^{t} N_i, t = 1,2,\cdots,n \quad (4)$$

$$\boldsymbol{X}(\boldsymbol{m}) = \sum_{i=1}^{t}\left(\Delta N_i - \overline{\Delta N(t)}\right), 1 \le m \le t \quad (5)$$

$$\boldsymbol{R}(\boldsymbol{t}) = \max_{1\le t\le n} X(m) - \min_{1\le t\le n} X(m), t = 1,2,\cdots,n \quad (6)$$

$$\boldsymbol{S}(\boldsymbol{t}) = \left[\frac{1}{t}\sum_{i=1}^{t}(\Delta N_i - \Delta\overline{N(t)})^2\right]^{\frac{1}{2}}, t = 1,2,\cdots,n \quad (7)$$

Where: the time series N_i is the annual mean rainfall erosive power in year *i*. For any positive integer t (t ∈ (0,∞]), the mean series of this time series is defined as $\overline{N(t)}$, The cumulative deviation is *X(m)*, The extreme deviation is R(t), The standard deviation is *S(t)*; ΔN_i and $\Delta\overline{N(t)}$ is the difference sequence, $\Delta N_i = N_i - N_{i-1}$, $\Delta\overline{N(t)} = \Delta\overline{N(t)} - \Delta\overline{N(t-1)}$. If exists, $R/S \propto t^H$, suggests the existence of the Hurst phenomenon in the time series Ni. H is the Hurst exponent, when $H<0.5$, it indicates that the time series is anti-persistent, when $0.5<H<1$, it indicates that the time series is persistent (Yin et al., 2022).

3) Biased correlation analysis

Partial correlation analysis is used to examine the correlation between two variables while excluding the effects of other variables. In this study, partial correlation analysis was used to analyse the relationship between rainfall erosivity and non-photosynthetic cover and livestock carrying capacity on the Qinghai-Tibet Plateau. The calculation formula is as follows:

$$\boldsymbol{R_{gh}} = \frac{\sum_{i=1}^{n}(g_i-\overline{g})(h_i-\overline{h})}{\sqrt{\sum_{i=1}^{n}(g_i-\overline{g})^2\sum_{i=1}^{n}(h_i-\overline{h})^2}} \quad (8)$$

$$\boldsymbol{R_{gh,k}} = \frac{R_{gh}-R_{gk}\times R_{hk}}{\sqrt{\left(1-R_{gk}^2\right)\left(1-R_{hk}^2\right)}} \quad (9)$$

$$\boldsymbol{R_{gh,kl}} = \frac{R_{gh,k}-R_{gl,k}\times R_{hl,k}}{\sqrt{\left(1-R_{gh,k}^2\right)\left(1-R_{hl,k}^2\right)}} \quad (10)$$

Where: R_{gh} is the correlation coefficient between the two variables. g_i and h_i are the values of g and h for year i, respectively; $\bar{g}$ and $\bar{h}$ are the mean values of g and h, respectively, for the time period studied. $R_{gh,k}$ is the partial correlation coefficient between the variables g and h for the control variable k, R_{gk} and R_{hk} are the results of the correlation coefficients corresponding to the variables respectively. $R_{gh,kl}$ is the partial correlation coefficient of variables g and h with control variables k and l, $R_{gl,k}$ and $R_{hl,k}$ are partial correlation coefficients controlling for fixed variables, respectively, $R_{gh,kl}>0$ indicates that the two variables are positively correlated, $R_{gh,kl}<0$ indicates a negative correlation between the two variables, with larger absolute values representing a closer correlation.

The t-test was chosen to test for significance with the following formula:

$$\boldsymbol{t} = \frac{R_{gh,kl}}{\sqrt{1-R_{gh,kl}^2}}\sqrt{n-m-1} \quad (11)$$

The results were classified into: significant positive correlation (r>0, P<0.05) and significant negative correlation (r<0, P<0.05).

4) Multiple regression residual analysis

Residual trend analysis is the most representative method for quantitatively distinguishing the relative contributions of changes in non-photosynthetic vegetation cover and livestock carrying capacity to changes in rainfall erosivity. This method effectively clarifies the relative contributions of these two factors and is suitable for long time-series analyses (Evans et al., 2004). The method assumes that rainfall erosivity is determined by changes in non-photosynthetic vegetation cover. It first establishes a relationship between annual rainfall erosivity and non-photosynthetic vegetation cover using ordinary least squares regression (OLS). The residuals of this equation are considered to represent the change in rainfall erosivity due to livestock load. A positive residual indicates that livestock load drives rainfall erosivity to worsen, while a negative residual indicates that rainfall erosivity improves. The specific equations are given below:

$$\boldsymbol{TR_{pred}} = a \times FG + \varepsilon \quad (12)$$

$$\boldsymbol{TR_{res}} = TR_{real} - TR_{pred} \quad (13)$$

Where: *pred*、*real*、*res* are the predicted, observed, and residual values of rainfall erosivity, respectively; *a* and *b* correspond to the regression coefficients of the non-photosynthetic vegetation cover and constant terms of the multiple regression model, respectively.

5) Determination of drivers of rainfall erosivity change and relative contribution analysis

$$\boldsymbol{r_1} = \frac{slope(TR_{pred})}{slope(TR_{real})} \times 100\% \quad (14)$$

$$\boldsymbol{r_2} = \frac{slope(TR_{res})}{slope(TR_{real})} \times 100\% \quad (15)$$

Where: r_1 represents the contribution of non-photosynthetic vegetation cover to the erosive power of rainfall on vegetation; r_2 represents the contribution of grassland livestock load to the erosive power of rainfall on vegetation, where $r_2>0$, $r_2=0$, and $r_2<0$ indicate that grassland livestock load has a positive, negative, and no effect on vegetation change, respectively. The relative contribution of each driver to changes in rainfall erosivity (Table 1).

Table 1 Determination of non-photosynthetic vegetation cover and livestock carrying capacity as drivers of precipitation erosivity on the Qinghai-Tibetan Plateau and calculation of their contribution rates

slope (TR_{real})	Driving force	Criteria for classifying drivers		Contribution of drivers / %	
		$slope$ (TR_{pred})	slope (TR_{res})	Non-photosynthetic vegetation cover	Livestock carrying capacity
>0	Non-photosynthetic vegetation cover versus livestock carrying capacity	>0	>0	r_1	r_2
	Non-photosynthetic vegetation cover	>0	<0	100	0

	Livestock carrying capacity	<0	>0	0	100
<0	Non-photosynthetic vegetation cover versus livestock carrying capacity	<0	<0	r_1	r_2
	Non-photosynthetic vegetation cover	<0	>0	100	0
	Livestock carrying capacity	>0	<0	0	100

Note: slope（TR_{real}）is the actual precipitation erosivity trend; slope（TR_{res}）is the trend in the impact of changes in livestock carrying capacity; $slope$（TR_{pred}） is the trend of change in the impact of non-photosynthetic vegetation cover.

3.3. Data Sources

In this paper, we utilized relevant data for the Tibetan Plateau from 2000 to 2019. Water quantity data were obtained from the ERA5-Land dataset (https://cds.climate.copernicus.eu), published by the European Union and the European Centre for Medium-Range Weather Forecasts, among other organizations. For the same period, rainfall erosivity (Zhang, 2022), non-photosynthetic vegetation cover (Niu, 2024), and grassland carrying capacity information (Liu, 2023) for the Tibetan Plateau region were sourced from the China Tibetan Plateau Science Data Centre (https://data.tpdc.ac.cn/). To ensure consistency in spatial data resolution, all raster data were resampled to a resolution of 500 m (0.5 KM × 0.5 KM). Rainfall erosivity was calculated from daily rainfall data using Kriging interpolation to generate raster maps. Non-photosynthetic vegetation cover was estimated by constructing a binary model based on MOD09A1, utilizing the normalized difference tillage index. Grassland livestock carrying capacity was determined using statistical yearbooks from each province (district) and city (state) on the Tibetan Plateau. This information was then combined with multiple linear regression analysis to produce actual livestock carrying capacity raster data. As noted by Zeng et al., ordinary least squares regression (OLS) estimation is sensitive to outliers (Zeng et al., 2025). Therefore, during data processing, we assigned 'Nodate' values to outlier rasters to mitigate this sensitivity.

4. Results

4.1 Characteristics and trends of rainfall erosivity on the Qinghai-Tibet Plateau

Based on the spatial and temporal distribution of rainfall erosive power on the Qinghai-Tibet Plateau (Figure 2), it can be seen that the rainfall erosive power in the region shows a fluctuating trend. It first increases, then decreases, and then increases again. However, the differences in hydrothermal conditions and vegetation types across different locations on the Qinghai-Tibet Plateau result in significant spatial heterogeneity in rainfall erosive power. This is evidenced by a gradual increase from the northwest to the southeast, forming a pole of high values in the southeast. Higher rainfall erosivity is concentrated in the southeastern part of the Qinghai-Tibet Plateau, while lower values are distributed in the central and northwestern parts.

To further analyse the evolution process of different rainfall erosive force degrees, we examined the spatial distribution of rainfall erosive force trend types (Figures 3 and 4). The rainfall erosive forces in the ranges of 0-200 ($MJ \cdot mm \cdot 0.25hm^2 \cdot h^{-1}$), 200-500 ($MJ \cdot mm \cdot 0.25hm^2 \cdot h^{-1}$), and 500-800 ($MJ \cdot mm \cdot 0.25hm^2 \cdot h^{-1}$) had the largest areas of change. The changes in rainfall erosivity for the 0-200 and 200-500 ($MJ \cdot mm \cdot 0.25hm^2 \cdot h^{-1}$) ranges were significant, and most of these areas were located in the southwest-northeast of the Qinghai-Tibet Plateau. From 2000 to 2010, the areas with rainfall erosivity in the 200-500 and 500-800 ($MJ \cdot mm \cdot 0.25hm^2 \cdot h^{-1}$) ranges gradually increased from the southeast to the northwest. Specifically, the area of 200-500 ($MJ \cdot mm \cdot 0.25hm^2 \cdot h^{-1}$) increased by 48.31% year-on-year compared to 2000, and the area of 500-800 ($MJ \cdot mm \cdot 0.25hm^2 \cdot h^{-1}$) increased by 70.25%. In contrast, the area of 0-200 ($MJ \cdot mm \cdot 0.25hm^2 \cdot h^{-1}$) decreased by 68.39% year-on-year. The rainfall erosivity from 2000 to 2019 exhibited an 'N' shape, with a sharp decrease in 2015 and a gradual recovery to the 2010 level by 2019.

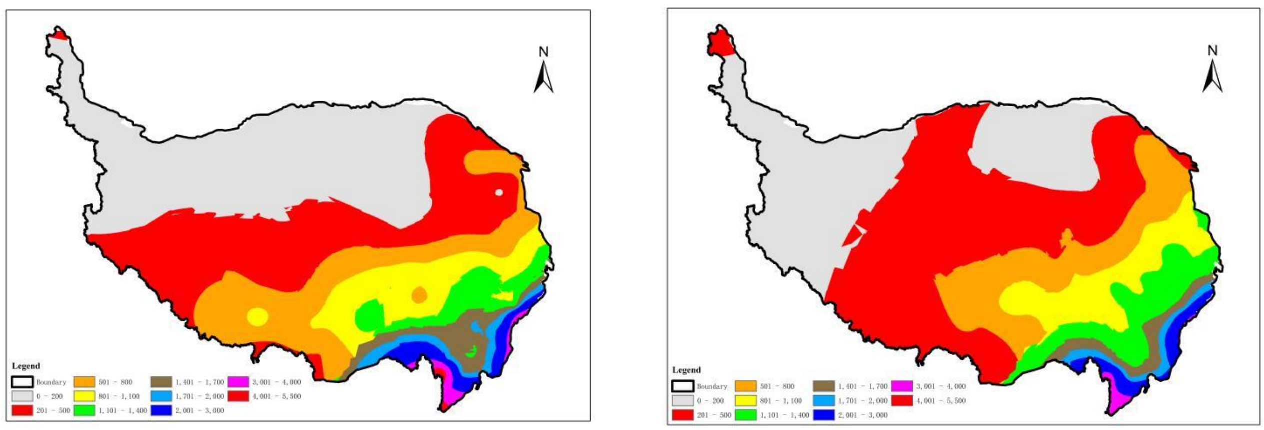

a b

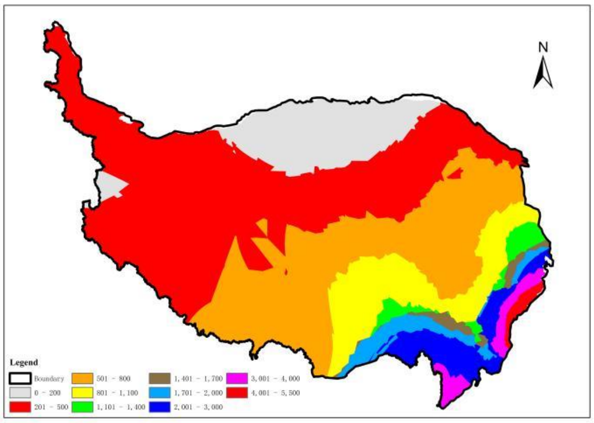

c

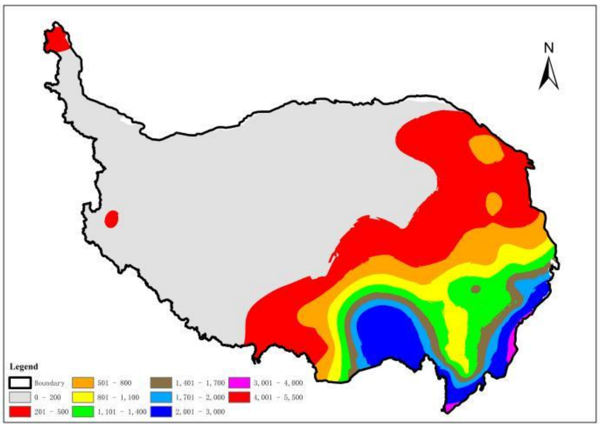

d

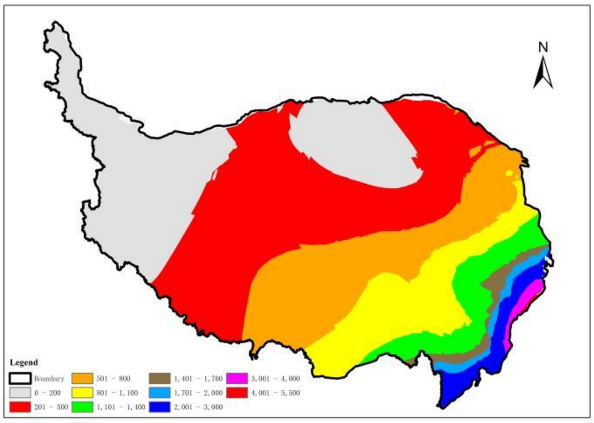

e

Figure 2 Temporal and spatial variation of rainfall erosive power on the Qinghai-Tibetan Plateau. (a) Rainfall erosive power distribution, 2000; (b) Rainfall erosive power distribution, 2005; (c) Rainfall erosive power distribution, 2010; (d) Rainfall erosive power distribution, 2015; (e) Rainfall erosive power distribution, 2019

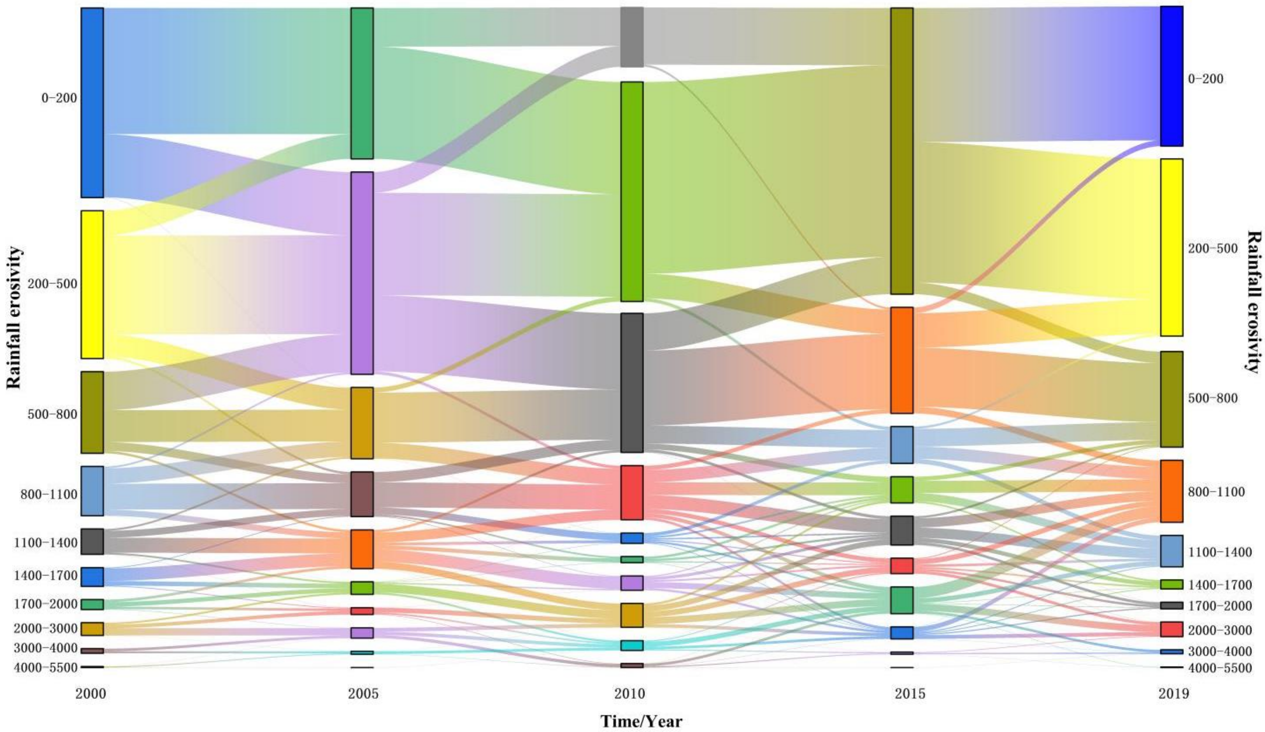

Figure 3 Mulberry map of rainfall erosive power on the Qinghai-Tibetan Plateau

The types of rainfall erosion changes on the Qinghai-Tibet Plateau showed significant regional heterogeneity from 2000 to 2019. Specifically, the area with an increasing trend in rainfall erosivity was dominated by a point-like distribution. This distribution was primarily concentrated in the east-central region and accounted for 5.96% of the entire study area. Within this increasing area, the proportion of non-significant increase was 57.88%. Meanwhile, the areas with decreasing trends in rainfall erosivity also demonstrated a point-like distribution. These areas were primarily concentrated in the northern region and covered 18.57% of the total study area. It is worth noting that among these decreasing trend areas, the phenomenon of very significant decreases was particularly prominent. These decreases were particularly concentrated in the northwestern steppe desert area, the southern foothills of the Qilian Mountains, and the northeastern part of Qinghai Lake. The proportion of very significant decreases in all regions with decreasing trends reached 58.53%. This indicates that China's conservation measures on the Qinghai-Tibet Plateau have achieved significant results, especially in curbing rainfall erosion.

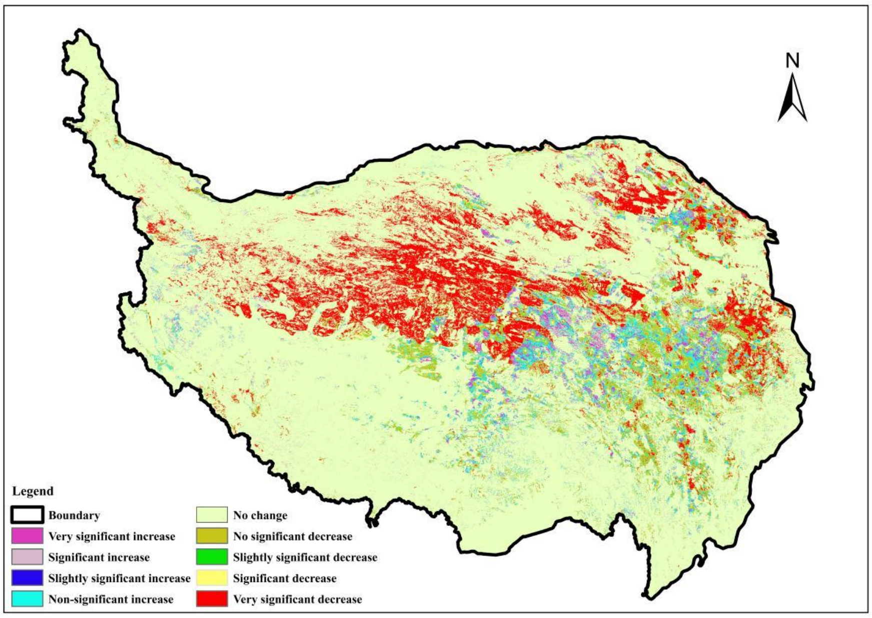

Figure 4 Spatial distribution of rainfall erosivity trends on the Qinghai-Tibet Plateau, 2000-2019

According to the data in Table 2, the percentage of the area with a Hurst index greater than 0.5 on the Qinghai-Tibet Plateau is 28.84%, while the percentage of the area with a Hurst index less than 0.5 is 71.16%. This indicates that the trend of rainfall erosivity is more inclined to be anti-persistent rather than persistent. Furthermore, the spatial distribution shown in Figure 5 indicates that the area with a potential degradation trend exceeds the area demonstrating a continuous improvement trend. The sustainability of the trend of change was assessed by coupling the magnitude of change in rainfall erosivity with the Hurst index in an overlay analysis using ArcMap 10.8. The results of the overlay statistics provided in Figure 6 and Table 2 showed that 53.731% of the areas across the study area exhibited an increasing trend in rainfall erosivity with a Hurst index of less than 0.5. This implies that despite the increase in rainfall erosivity in these areas, their future trend of change is not significantly correlated with historical patterns, indicating anti-sustainability. In contrast, 24.154% of the areas showed both increasing rainfall erosivity and a Hurst index above 0.5, suggesting a persistent degradation trend in these areas. Additionally, 4.687% of the areas were classified as continuously improving, while 17.428% were classified as reverse continuously improving. Overall, the percentage of the area within the Qinghai-Tibet Plateau that showed weak or weaker persistence was as high as 84.157%, indicating that the region as a whole experienced a weaker but stable degradation trend.

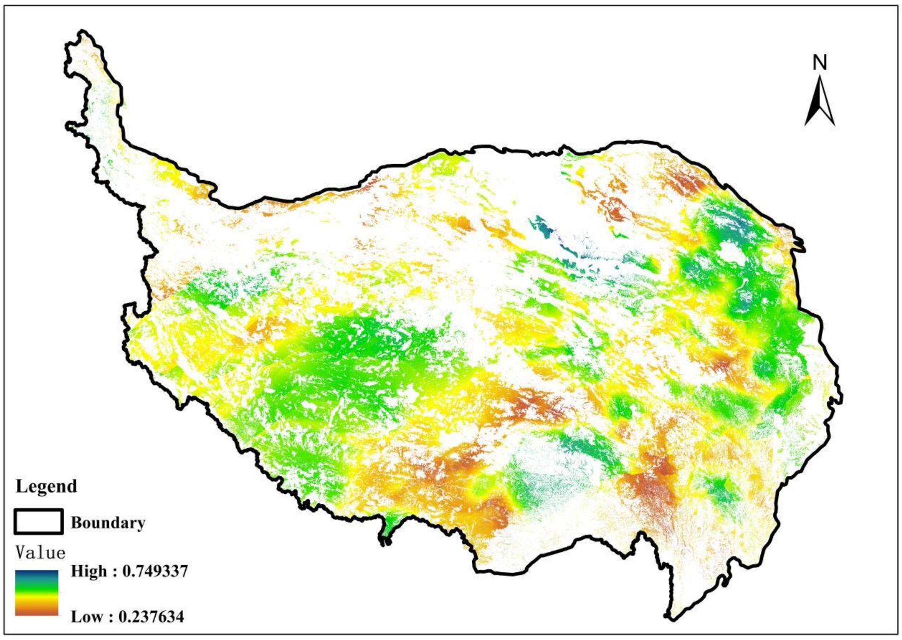

Figure 5 Spatial distribution of the Hurst index on the Qinghai-Tibetan Plateau

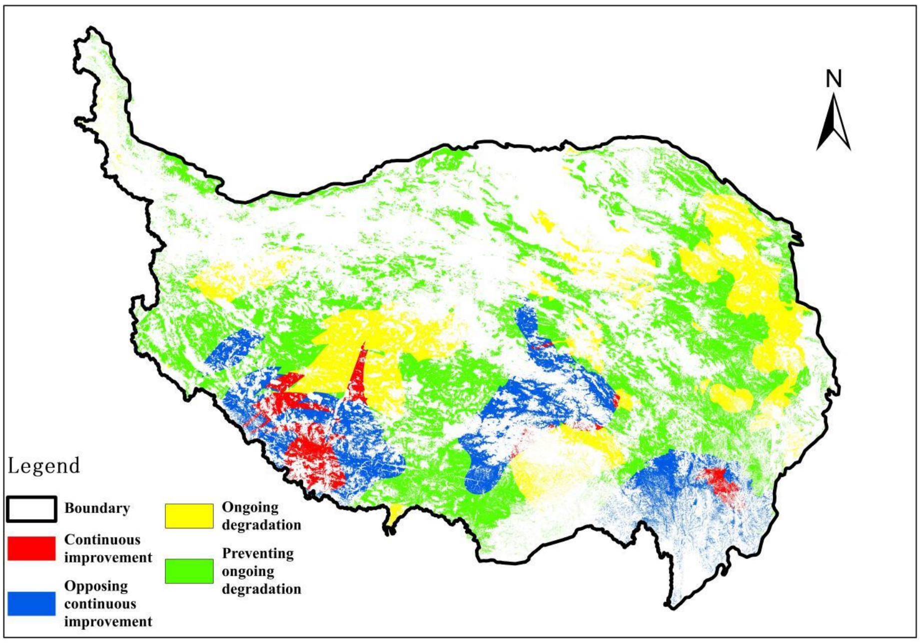

Figure 6 Spatial distribution of the persistence region of rainfall erosivity trends on the Qinghai-Tibetan Plateau

Table 2 Area share of persistent areas of rainfall erosivity trends on the Qinghai-Tibetan Plateau 286

Magnitude of change in rainfall erosivity (Q)	Hurst Index (H)	Changes in rainfall erosivity	Number of pixels / Pc	Area share / %

$Q > 0$	$H > 0.5$	Continual improvement	919904	8.83%
$Q > 0$	$H < 0.5$	Opposing continuous improvement	2046355	19.65%
$Q < 0$	$H > 0.5$	Continual improvement	178510	1.71%
$Q < 0$	$H < 0.5$	Preventing Ongoing degradation	663725	6.37%

4.2 Analysis of the mechanisms driving changes in rainfall erosivity on the Qinghai-Tibet Plateau

Significant correlations ($P < 0.05$) existed between rainfall erosivity and non-photosynthetic vegetation cover as well as grassland carrying capacity on the Qinghai-Tibet Plateau, as shown in Figures 8 and 9 and Table 3. Specifically, the relationship between non-photosynthetic vegetation cover and rainfall erosive power exhibited spatial heterogeneity. In the central Qinghai-Tibet Plateau, the two showed a significant positive correlation, with a likelihood of 1.48% in these regions. This positive correlation was sporadically distributed throughout the plateau. On the contrary, in the southern and northeastern Qinghai-Tibet Plateau, there was a significant negative correlation between non-photosynthetic vegetation cover and rainfall erosivity. Although these negative correlations were more concentrated, the pixel share was 2.40%. For the effect of changes in grassland carrying capacity, it was observed thatthe relationship between it and rainfall erosivity also showed a complex spatial pattern. Positive and negative correlations were interspersed in the center of the Plateau, as well as in multiple independent points in the southwestern and northeastern parts of the Plateau. These areas also accounted for 2% of the total number of pixels.

Overall, the correlations between rainfall erosivity and non-photosynthetic vegetation cover on the Qinghai-Tibet Plateau show both positive and negative patterns. These patterns are predominantly observed in the southwestern and northeastern parts of the plateau. The Tanggula Mountains serve as the axis of symmetry.

Compared with the effect of changes in pasture loading on rainfall erosivity, the effect of non-photosynthetic vegetation cover was more significant. This significance was evident in both a wider range and statistical significance. The number of pixels with a significant positive correlation was 41.86% higher than those with pasture loading, and the number of pixels with a significant negative correlation was 52.40% higher

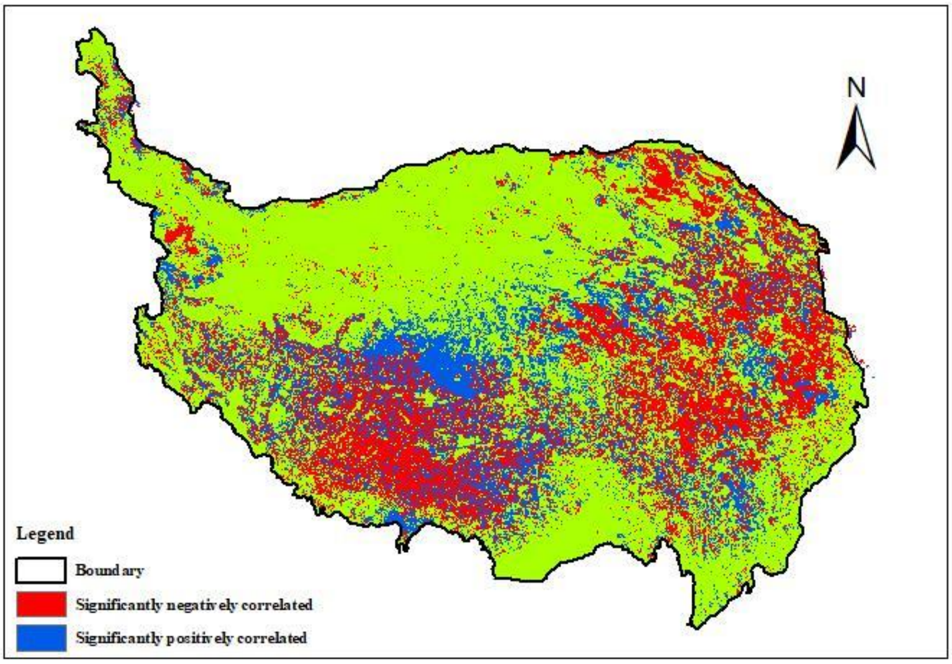

Figure 7 Spatial distribution of areas of biased correlation between non-photosynthetic vegetation cover and rainfall erosivity on the Qinghai-Tibetan Plateau

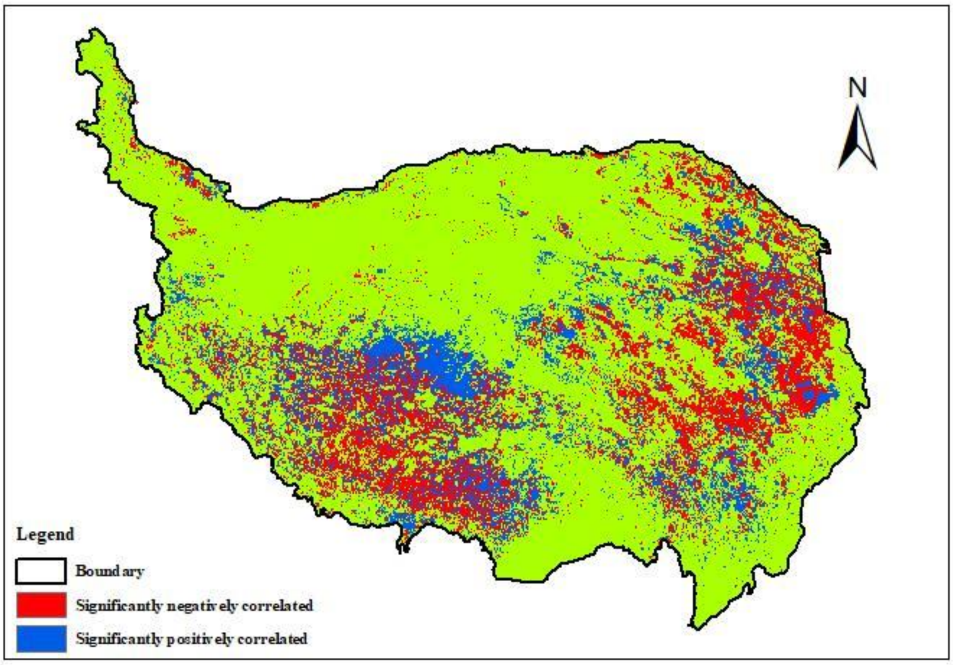

Figure 8 Spatial distribution of areas with biased correlation between livestock carrying capacity and rainfall erosivity correlation on the Qinghai-Tibetan Plateau

Table 3 Area share of non-photosynthetic vegetation cover and livestock carrying capacity in relation to the erosive power of precipitation on the Qinghai-Tibetan Plateau

Partial correlation coefficient	Non-photosynthetic vegetation cover		Livestock carrying capacity	
	Number of pixels / Pc	Area share / %	Number of pixels / Pc	Area share / %
Significant positive correlation	154261	1.48%	89683	0.86%
Significantly negative correlation	249808	2.40%	118905	1.14%

As shown in Figure 9 and Table 4, 17.66% of the Qinghai-Tibet Plateau is negatively driven by non-photosynthetic vegetation cover and grassland carrying capacity. In contrast, only 3.07% is positively driven by these factors. Additionally, 1.63% of the area is negatively driven solely by non-photosynthetic vegetation cover. The proportion of areas where rainfall erosion is reduced only by positive non-photosynthetic vegetation cover is 0.15%. This area is adjacent to the region where rainfall erosion is increased only by negative non-photosynthetic vegetation cover, and the distribution is relatively dispersed. The proportion of the area with increased rainfall erosivity driven only by pasture loading was 9.27%. This area was distributed across the Qinghai-Tibet Plateau, excluding certain regions such as parts of the Hengduan Mountain Range in the southeast and portions of Rikaze City in the Tibet Autonomous Region. In contrast, the proportion of the area with decreased rainfall erosivity driven only by positive grass loading was 4.85%. This distribution was the opposite of the areas with increased rainfall erosivity driven only by pasture loading on the Qinghai-Tibet Plateau. Overall, non-photosynthetic vegetation cover and grassland stocking together dominantly drove the increased in rainfall erosivity risk on the Qinghai-Tibet Plateau.

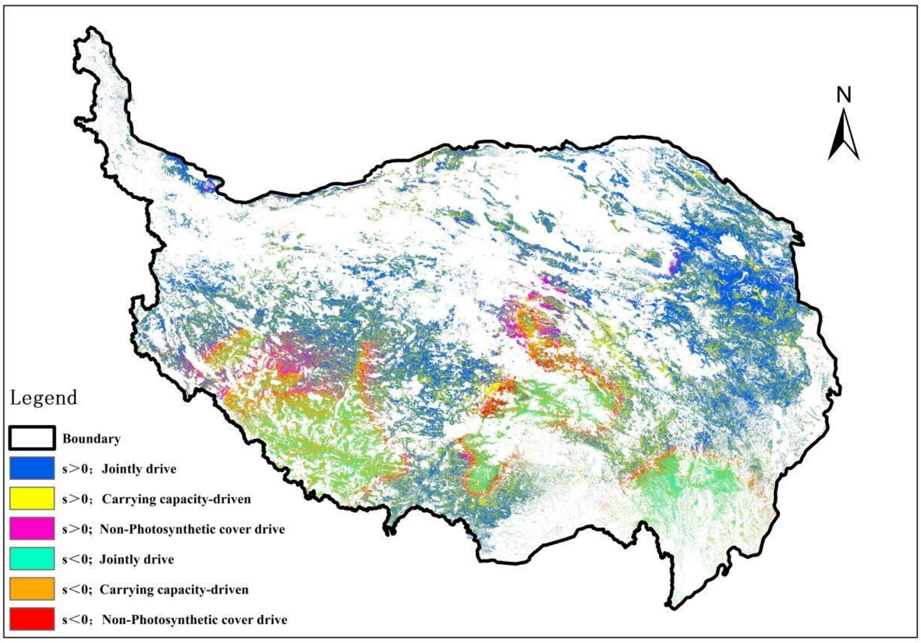

Figure 9 Spatial distribution of drivers of rainfall erosion changes on the Qinghai-Tibetan Plateau

Table 4 Area share of drivers of rainfall erosion change on the Qinghai-Tibet Plateau

Trends in rainfall erosion	Driving force	Number of pixels / Pc	Area share / %
Rainfall erosion＜0	Co-Driven	320720	3.07%
	Non-photosynthetic vegetation cover	88278	0.85%
	Livestock carrying capacity	433236	4.15%
Rainfall erosion＞0	Co-Driven	1843021	17.66%
	Non-photosynthetic vegetation cover	170342	1.63%
	Livestock carrying capacity	967885	9.27%

4.3 Relative contribution of different drivers to changes in rainfall erosivity of vegetation

Residual analyses were used to distinguish the relative contributions of non-photosynthetic vegetation cover and grassland carrying capacity to changes in rainfall erosivity on the Qinghai-Tibet Plateau. As shown in Figure 10, the percentage of the area with a positive contribution of non-photosynthetic vegetation cover to the change in rainfall erosion reduction was 17.58%, while the percentage with a negative contribution was 19.33% (Figure 10, Table 5). Among these, the contribution of non-photosynthetic vegetation cover ranged from -20% to 20%, accounting for a larger area of 25%. The percentage of the area contributing to the decrease in rainfall erosion on the Qinghai-Tibet Plateau was 9.72%, and the percentage of the area contributing to the increase in rainfall erosion was 26.99%. The area with a contribution rate of ≥80% accounted for 20.01% of the total area of the Qinghai-Tibet Plateau. According to the comparison results, non-photosynthetic vegetation cover and the amount of livestock on grassland have different contributions to changes in rainfall erosivity on the Qinghai-Tibet Plateau. The relative negative contribution of the amount of livestock on grassland was 26.99%. This is significantly higher than the 17.38% contribution of non-photosynthetic vegetation cover.Therefore, the effect of non-photosynthetic vegetation cover on reducing rainfall erosion on the Qinghai-Tibet Plateau was greater than that of the amount of livestock on grassland.

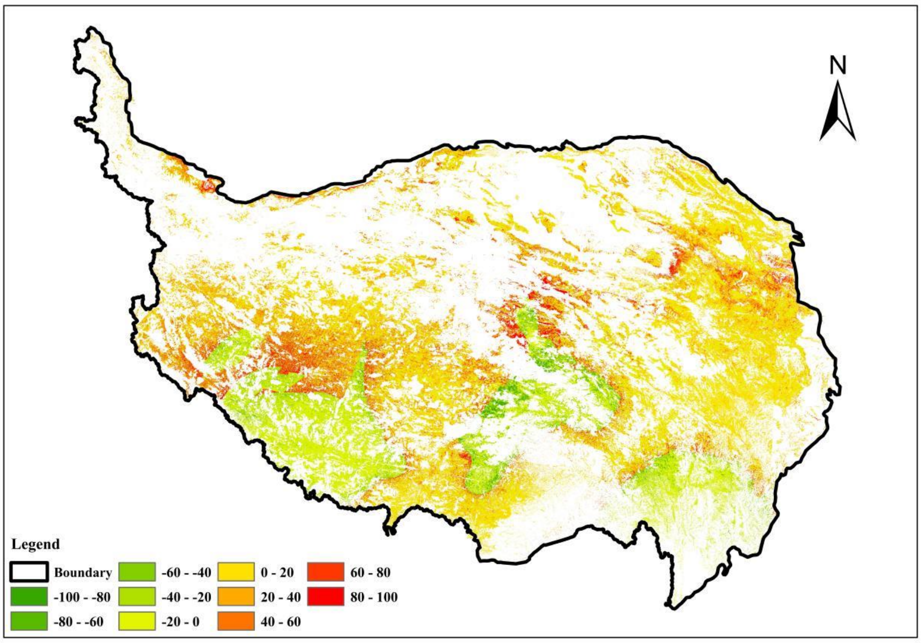

Figure 10 Spatial distribution of the contribution of non-photosynthetic vegetation cover to changes in rainfall erosivity on the Qinghai-Tibetan Plateau

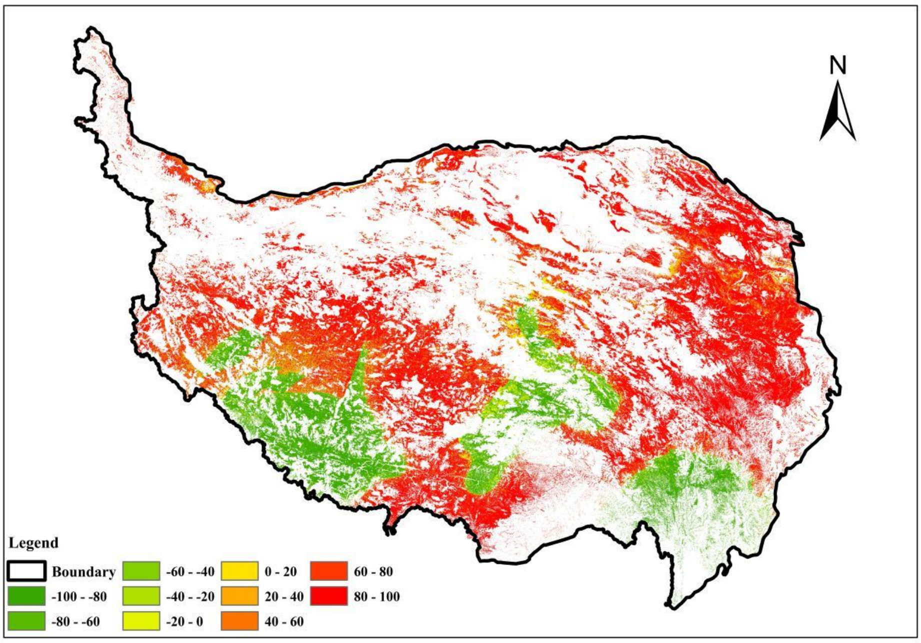

Figure 11 Spatial distribution of the contribution of non-photosynthetic vegetation cover to changes in rainfall erosivity on the Qinghai-Tibetan Plateau

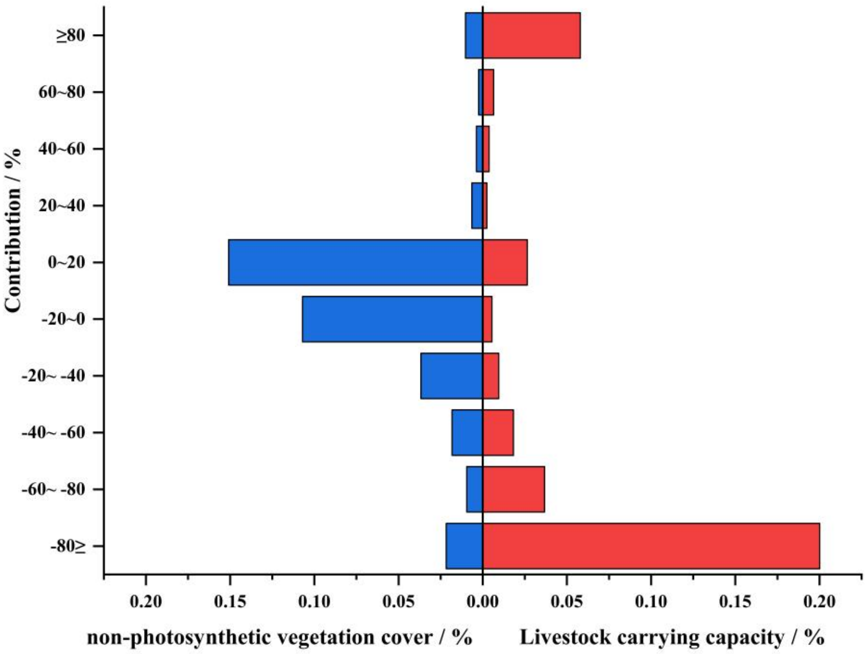

Figure 12 Area share of changes in non-photosynthetic vegetation cover and livestock carrying capacity in relative contribution to changes in rainfall erosion reduction on the Qinghai-Tibetan Plateau

5. Discussion

5.1 Spatial and temporal trends in rainfall erosivity on the Qinghai-Tibet Plateau

Rainfall erosivity can quantitatively characterise the ability of surface soil to be physically eroded by precipitation and is widely used as a proxy indicator of soil water retention and erosion. The changes in rainfall erosivity on the Qinghai-Tibet Plateau from 2000 to 2019 show non-stationary fluctuations. The spatial pattern demonstrates a distribution characterized by high values in the southeast and low values in the northwest. This is consistent with the findings of Gu et al., (2020) who reported a significant decreasing trend in rainfall erosivity from southeast to northwest on the Qinghai-Tibet Plateau. The middle and high value areas (rainfall erosivity > 200 ($MJ\cdot mm\cdot 0.25hm^2\cdot h^{-1}$)) are concentrated and continuously distributed in the southeastern part of the Qinghai-Tibet Plateau. This distribution is in remarkable consistency with the precipitation pattern of the Qinghai-Tibet Plateau. The reason for this is that the distribution of different erosion types on the Qinghai-Tibet Plateau varies, with hydraulic erosion dominating in the eastern region and deep-freeze erosion dominating in the central and western regions. The dividing line between the two constitutes a significant low value area (rainfall erosivity < 200 ($MJ\cdot mm\cdot 0.25hm^2\cdot h^{-1}$)) and a medium-high value area (rainfall erosivity > 200 ($MJ\cdot mm\cdot 0.25hm^2\cdot h^{-1}$)), as shown in Figure 13. Secondly, the eastern part of the Qinghai-Tibet Plateau is influenced by the summer southwest monsoon and receives relatively high levels of precipitation. In contrast, the northwest region, far from the ocean and in the rain shadow zone, receives less precipitation. Surface soils in the eastern part are more frequently exposed to rainfall, increasing the erosive power of rainfall (Dash et al., 2024). Thirdly, the eastern region of the Qinghai-Tibet Plateau is located at the confluence of China's first and second topographic steps. The complex terrain in this area promotes rapid surface runoff formation. Steeper slopes further increase the potential for rainfall erosion (Liu et al., 2024). The northwestern part of the plateau or the more gentle hilly areas have a relatively slow water flow rate, which reduces the risk of erosion. This effectively suppresses the momentum of the westward expansion of rainfall erosive force on the Qinghai-Tibet Plateau, as shown in Figure 14. This finding is consistent with other scholars' studies, which indicate that land slope, rainfall, and other factors are related to rainfall erosion (Bai et al., 2024; Guerrero-Campo et al., 1999).

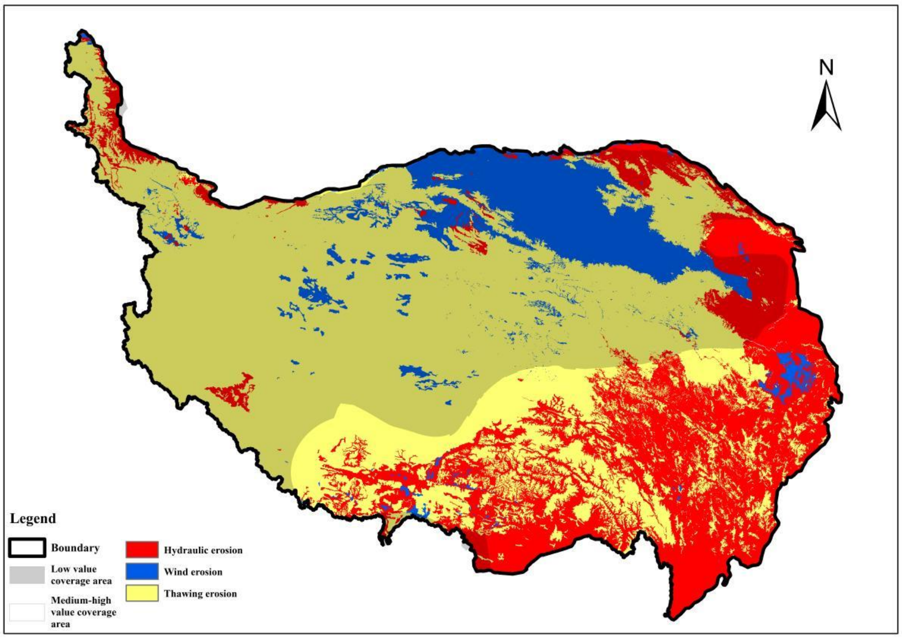

Figure 13 Overlap of the distribution of different values of precipitation erosivity with the distribution of different erosion types on the Qinghai-Tibetan Plateau

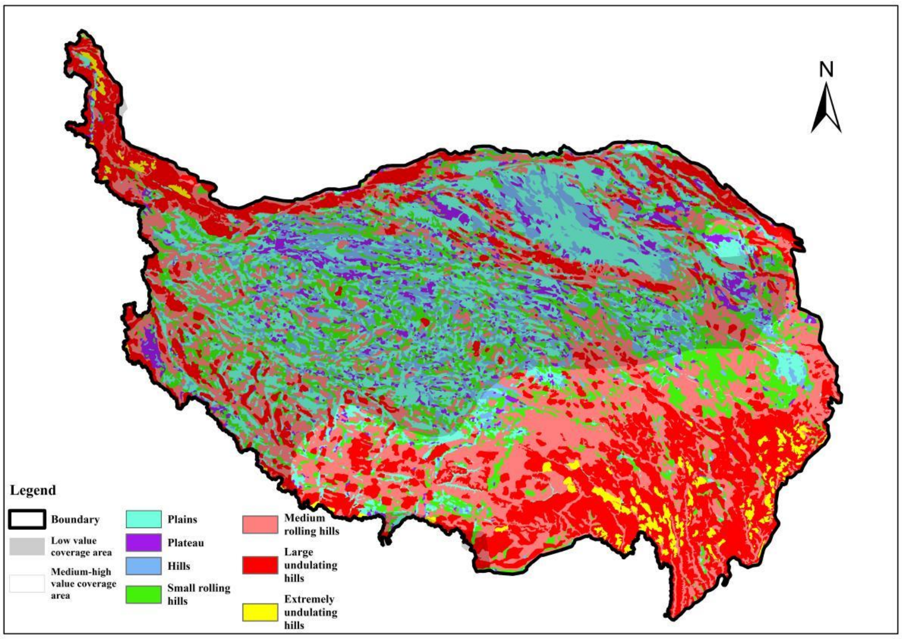

Figure 14 Overlap of the distribution of different values of precipitation erosivity with the distribution of different landform types on the Qinghai-Tibetan Plateau

There are interannual fluctuations in temporal changes, showing the dynamics of the middle and high value zones (rainfall erosive power > 200 (MJ·mm·0.25hm²·h⁻¹)) migrating from southeast to northwest and then returning and migrating again. The reasons for these fluctuations may be related to the establishment of regional ecological protection zones, the implementation of ecological restoration projects, yearly differences, and climatic fluctuations (Figure 15). This is consistent with the positive correlation between rainfall erosivity and mean annual precipitation found by Capolongo et al (Capolongo et al., 2008). However, contrary to the results of Yuan et al., (2021) who showed no significant effect of rainfall intensity on soil erosion, the possible reason may be due to the selected vegetation cover with regional variability. This suggests that the specific type and distribution of vegetation cover can influence the relationship between rainfall intensity and soil erosion. The results of the persistence analyses show that the future evolution of rainfall erosivity on the Qinghai-Tibet Plateau exhibits strong anti-persistence. This increases the risk of a potential rise in erosivity due to continued overloading of livestock carrying capacity. Characterizing future changes in rainfall erosivity, spatial distribution differences, and temporal variations can provide a theoretical foundation for major ecological restoration assessments and future vegetation protection policy formulation. These analyses can also be used to evaluate the rationality of new ecological protection policies.

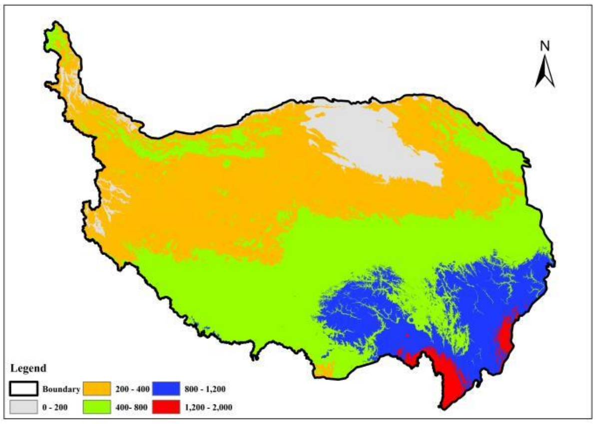

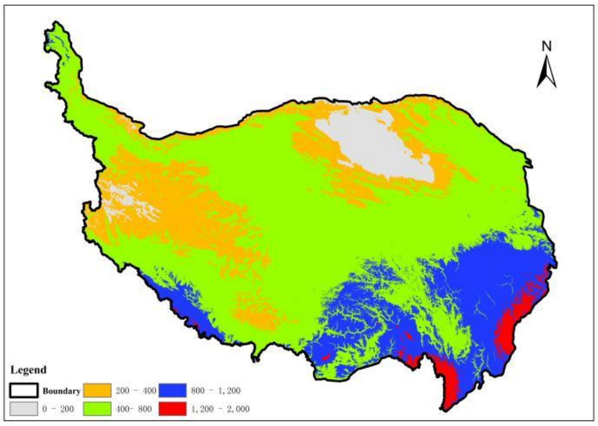

a

b

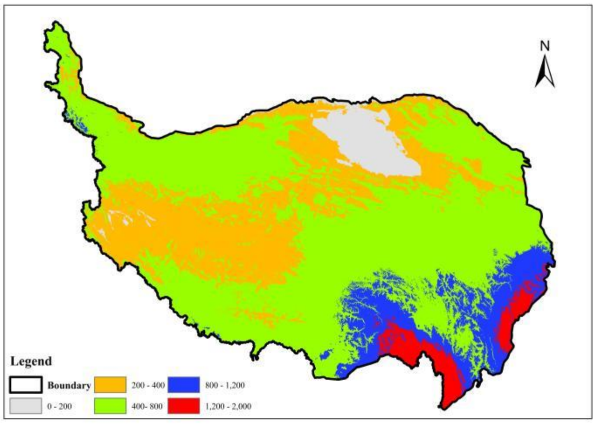

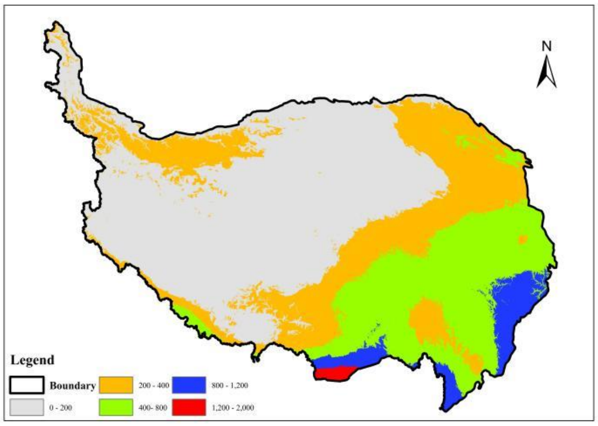

c

d

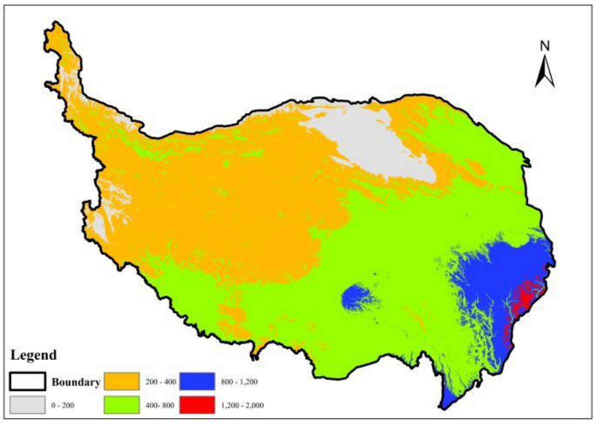

e

Figure 15 Temporal and spatial variability of precipitation on the Qinghai-Tibetan Plateau. (a) Rainfall distribution, 2000; (b) Rainfall distribution, 2005; (c) Rainfall distribution, 2010; (d) Rainfall distribution, 2015; (e) Rainfall distribution, 2019

5.2 Analysis of the driving mechanism of rainfall erosivity dynamics on the Qinghai-Tibet Plateau

Non-photosynthetic vegetation cover and grassland carrying capacity were the basic drivers affecting the spatial distribution of rainfall erosivity and its changes. In this study, changes in non-photosynthetic vegetation cover had a low driving force for the reduction in rainfall erosivity and high explanatory power for the spatial distribution of the increase in rainfall erosivity. This drove 1.63% of the increase in rainfall erosivity on the Qinghai-Tibet Plateau. Correlation analyses of year-to-year rainfall erosivity with non-photosynthetic vegetation cover and grassland carrying capacity verified these findings. The results suggest that non-photosynthetic vegetation cover is not conducive to suppressing rainfall erosivity from precipitation. This is not in line with the assertion by Yuan et al. (2021) that reasonable cropping patterns have little effect on soil runoff generation. The partial correlation analysis showed that rainfall erosivity and livestock carrying capacity were significantly positively correlated at the 1% significance level from 2000 to 2019. However, they were less significantly negatively correlated during the same period.

Livestock carrying capacity had an important effect on the change in rainfall erosivity on the Qinghai-Tibet Plateau from 2000 to 2019. Livestock carrying capacity had a positive effect on rainfall erosivity, and the percentage of the area where the change in rainfall erosivity was less inhibitory than facilitatory due to the livestock carrying capacity of grassland was 9.27%. According to Figure 16, it can be observed that pixels representing precipitation erosivity between 0 - 500 ($MJ \cdot mm \cdot 0.25hm^{2} \cdot h^{-1}$) overlap with pixels indicating grassland carrying capacity that is not overloaded. These overlaps were analyzed Using software （ArcMap 10.8）. Spatial intersection ratios were calculated for all precipitation erosivity pixels, revealing that the overlap exceeded 20% from 2000 to 2019. Similarly, pixels representing precipitation erosivity between 500 - 1100 ($MJ \cdot mm \cdot 0.25hm^{2} \cdot h^{-1}$) were overlaid with pixels showing areas of general overloading in livestock carrying capacity. Using software （ArcMap 10.8）, spatial intersection ratios were computed for all precipitation erosivity pixels, resulting in overlap ratios exceeding 12% across all years from 2000 to 2019. These findings indicate that reasonable grazing has an inhibitory effect on grassland precipitation erosion, while overloaded grazing positively contributes to the erosive power of precipitation in grassland (Vîrghileanu et al., 2024). The spatial distribution of the increase in rainfall erosivity in the southwestern and northeastern zones of the Qinghai-Tibet Plateau is affected by the coupling of non-photosynthetic vegetation cover and grassland overstocking. This coupling leads to a significant increase in rainfall erosivity and an expansion of soil erosion and soil nutrient depletion. With the implementation of large-scale ecological projects and the forbidden grazing policy, the use of grassland has become more rational. The degradation of grassland has been curbed, and the negative impact of grassland overloading on the erosive power of rainfall on the Qinghai-Tibet Plateau has gradually weakened. In some areas, such as the mining area in the Qaidam Basin, changes in rainfall erosivity are mainly influenced by anthropogenic disturbances. Long-term and rapidly expanding mining activities have caused serious problems, including land depressions and damage to geomorphic landscapes. These issues result in weaker stability of the vegetation cover and similar problems such as land desertification and soil erosion. It is necessary to further strengthen the control of the amount of livestock carried on grassland and to coordinate the relationship between economic development and environmental protection.

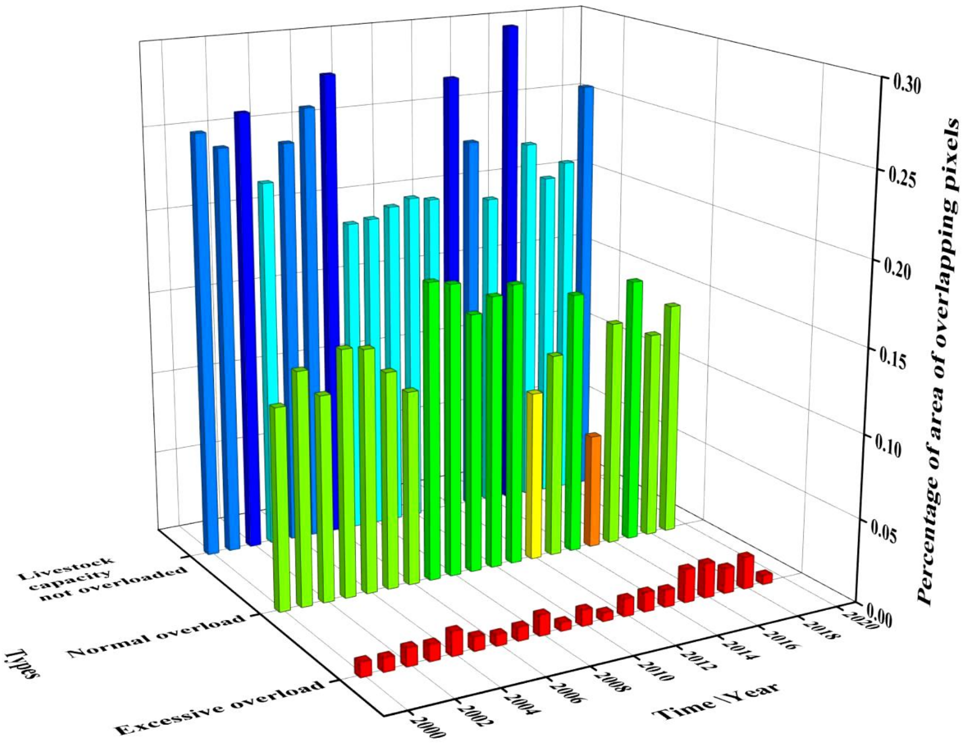

Figure 16 Area share of overlapping pixels for changes in livestock carrying capacity of precipitation erosion force grassland on the Qinghai-Tibetan Plateau

5.3 Relative contribution of non-photosynthetic vegetation cover to grassland livestock carrying capacity 417

Non-photosynthetic vegetation cover is a key control element in suppressing the erosive power of precipitation. However, the implementation of a series of ecological restoration projects has also played an important role in the rapid recovery of non-photosynthetic vegetation cover (Liu et al., 2024). Given the spatial heterogeneity of non-photosynthetic vegetation cover and grassland carrying capacity, there is notable spatial variation in their contribution to the erosive impact of precipitation. Higher non-photosynthetic vegetation cover reduces direct soil contact with precipitation, thereby reducing the direct impact of rainfall on the soil. Higher vegetation cover also tends to allow rainfall to form impactful water flows that cause secondary impacts on the soil. Light grazing maintains both grassland health, soil structure, and normal vegetation cover. Overgrazing, however, directly reduces vegetation cover, indirectly reduces dead leaves, and over-trampling breaks down soil structure, increasing the area of soil in contact with rainfall and reducing soil resilience (Donovan, 2022).

6.Conclusion and policy implications

6.1 Conclusion

This paper examines how non-photosynthetic vegetation cover and livestock carrying capacity influence rainfall erosivity on the Tibetan Plateau. The investigation is based on two scenarios: the spatial correlation among these factors and the overlay of regional heterogeneity. To achieve this, the study employed a combination of geospatial regression analyses and statistical tests. The primary findings are summarized as follows: (1) From 2000 to 2019, the rainfall erosivity on the Qinghai-Tibet Plateau showed a fluctuating trend. It followed an 'N'-shaped pattern: first increasing, then decreasing, and then increasing again. The spatial distribution exhibited a gradual increasing trend from northwest to southeast. (2) There is a significant correlation between rainfall erosivity, non-photosynthetic vegetation cover, and grassland livestock load on the Qinghai-Tibet Plateau, but the spatial heterogeneity is pronounced. Non-photosynthetic vegetation cover was significantly positively correlated in the central part of the Qinghai-Tibet Plateau, while it was significantly negatively correlated in the southern and northeastern parts. The influence of changes in livestock quantity on rainfall erosivity showed a more complex spatial pattern. Positive and negative correlation areas were staggered across the central plateau, as well as in the southwestern and northeastern parts. (3) Non-photosynthetic vegetation cover and grassland carrying capacity together drive 17.66% of the Qinghai-Tibet Plateau, making it the main factor for the increase in rainfall erosivity. The proportion of the area positively driven to decrease by these two factors alone was only 3.07%. This places the Qinghai-Tibet Plateau at risk of an overall increase in rainfall erosivity. (4) The relative contributions of non-photosynthetic vegetation cover and grassland carrying capacity to changes in rainfall erosivity on the Qinghai-Tibet Plateau were different. Grassland carrying capacity contributed significantly more to the increase in rainfall erosivity compared to non-photosynthetic vegetation cover. However, non-photosynthetic vegetation cover played a more significant role in reducing rainfall erosivity.

6.2 policy implications

According to the governance logic, we can break it down into three steps: identifying spatial differentiation, regulating key processes, and enhancing human intervention. Based on this logic, we propose the following policies. These policies address the special surface process mechanism of the Qinghai-Tibet Plateau and meet the strategic demand for constructing the national ecological security barrier. (1) The government should demonstrate foresight and take precedence in identifying the degree of rainfall erosion. They need to distinguish between key areas affected by rainfall erosion. Combining high-resolution remote sensing with monitoring, they should establish an early warning system for erosion. (2) The government should establish an early warning system for erosion. This system should integrate high-resolution remote sensing monitoring. (3) Develop compensation mechanisms for grass-animal balance according to regional characteristics. These mechanisms should aim to raise the income of herdsmen, thereby increasing their incentive to protect pastures. (4) Implement a red line system for the carrying capacity of grasslands. Limit the intensity of grazing during the rainy season to reduce the risk of exposing topsoil. Additionally, restrict the number of livestock to no more than 50% of the net primary productivity for summer rangelands and 30% for winter rangelands. (5) Improve the accuracy of climate change forecasting. Enhance the ability to regulate rainfall artificially.

Additionally, this paper has certain limitations: 1. The raster data used in this study is collected annually, making it impossible to accurately measure soil erosion caused by extreme rainfall events within a year. 2.Given that the study area is vast and geographically heterogeneous, further investigation is required to validate the applicability of our findings to smaller regions. 3.Due to the absence of data from some Tibetan Plateau forbidden grazing areas, we were unable to account for the livestock carrying capacity in these specific zones.

References

Abd Aziz, S., Steward, B. L., Kaleita, A. & Karkee, M. (2012). ASSESSING THE EFFECTS OF DEM UNCERTAINTY ON EROSION RATE ESTIMATION IN AN AGRICULTURAL FIELD. *Transactions of the Asabe*, *55*(3), 785-798.

Alves, A., Cogo, N. & Levien, R. (1995). Relationships between soil erosion and the persistence of dead plant cover.

Angulo-Martínez, M., Beguería, S., Navas, A. & Machín, J. (2012). Splash erosion under natural rainfall on three soil types in NE Spain. *Geomorphology*, *175*, 38-44.

Bai, Q. Q., Wang, L. & Cidan, Y. Z. (2024). Spatial and Temporal Variability of Rainfall Erosivity in the Niyang River Basin. *Atmosphere, 15*(9).

Busnelli, J., Neder, L. D. & Sayago, J. M. (2006). Temporal dynamics of soil erosion and rainfall erosivity as geoindicators of land degradation in Northwestern Argentina. *Quaternary International, 158*, 147-161.

Capolongo, D., Diodato, N., Mannaerts, C. M., Piccarreta, M. & Strobl, R. O. (2008). Analyzing temporal changes in climate erosivity using a simplified rainfall erosivity model in Basilicata (southern Italy). *Journal of Hydrology, 356*(1-2), 119-130.

Chang, Y. M., Lei, H. M., Zhou, F. & Yang, D. W. (2022). Spatial and temporal variations of rainfall erosivity in the middle Yellow River Basin based on hourly rainfall data. *Catena, 216*.

Chen, Y. L., Duan, X. W., Ding, M. H., Qi, W., Wei, T., Li, J. D. & Xie, Y. (2022). New gridded dataset of rainfall erosivity (1950-2020) on the Tibetan Plateau. *Earth System Science Data, 14*(6), 15.

Chen, Y. L., Duan, X. W., Zhang, G., Ding, M. H. & Lu, S. J. (2022). Rainfall erosivity estimation over the Tibetan plateau based on high spatial-temporal resolution rainfall records. *International Soil and Water Conservation Research, 10*(3), 422-432.

Cogo, N. P., Levien, R. & Schwarz, R. A. (2003). Soil and water losses by rainfall erosion influenced by tillage methods, slope-steepness classes, and soil fertility levels. *Revista Brasileira De Ciencia Do Solo, 27*(4), 743-753.

Cui, B. H., Zhang, Y. L., Liu, L. S., Xu, Z. H., Wang, Z. F., Gu, C. J., .&. Gong, D. Q. (2021). Spatiotemporal Variation in Rainfall Erosivity and Correlation with the ENSO on the Tibetan Plateau since 1971. *International Journal of Environmental Research and Public Health, 18*(21).

Das, S. & Jain, M. K. (2023). Unravelling the future changes in rainfall erosivity over India under shared socio-economic pathways. *Catena, 232*, 107417.

Dash, C. J., Shrimali, S. S., Madhu, M., Kumar, R. & Adhikary, P. P. (2024). Unveiling rainfall and erosivity dynamics in Odisha's varied agro-climatic zones for sustainable soil and water conservation planning. *Theoretical and Applied Climatology, 155*(8), 7557-7574.

Dong, S. K., Shang, Z. H., Gao, J. X. & Boone, R. B. (2020). Enhancing sustainability of grassland ecosystems through ecological restoration and grazing management in an era of climate change on Qinghai-Tibetan Plateau. *Agriculture Ecosystems & Environment, 287*.

Donovan, M. (2022). Modelling soil loss from surface erosion at high-resolution to better understand sources and drivers across land uses and catchments; a national-scale assessment of Aotearoa, New Zealand. *Environmental Modelling & Software, 147*.

Evans, J. & Geerken, R. (2004). Discrimination between climate and human-induced dryland degradation. *Journal of Arid Environments, 57*(4), 535-554.

Fan, J. R., Chen, Y., Yan, D. & Guo, F. F. (2013). Characteristics of rainfall erosivity based on tropical rainfall measuring mission data in Tibet, China. *Journal of Mountain Science, 10*(6), 1008-1017.

Fan, J. W., Shao, Q. Q., Liu, J. Y., Wang, J. B., Harris, W., Chen, Z. Q., & Liu, R. G. (2010). Assessment of effects of climate change and grazing activity on grassland yield in the Three Rivers Headwaters Region of Qinghai-Tibet Plateau, China. *Environmental Monitoring and Assessment, 170*(1-4), 571-584.

Feng, Y., Wang, N., Xie, H., Li, J., Li, G., Xue, L. & Chen, D. (2023). Livestock manure-derived hydrochar is more inclined to mitigate soil Global Warming Potential than raw materials based on soil stoichiometry analysis. *Biology and Fertility of Soils, 59*, 459-472.

Gao, H., Pang, G., Li, Z. & Cheng, S. (2017). Evaluating the potential of vegetation restoration in the Loess Plateau. *Acta Geographica Sinica, 72*(5), 863-874.

Gu, Z. J., Feng, D. T., Duan, X. W., Gong, K. F., Li, Y. W. & Yue, T. Y. (2020). Spatial and Temporal Patterns of Rainfall Erosivity in the Tibetan Plateau. *Water, 12*(1).

Guerrero-Campo, J., Alberto, F., Hodgson, J., García-Ruiz, J. M. & Montserrat-Martí, G. (1999). Plant community patterns in a gypsum area of NE Spain.: I.: Interactions with topographic factors and soil erosion. *Journal of Arid Environments, 41*(4), 401-410.

He, J., Wan, Y.-R., Chen, H.-T. & Wang, S.-L. (2022). Effects of Land Use Change on Rainfall Erosion in Luojiang River Basin, China. *Sustainability, 14*(14), 8441.

Huang, L., Cao, W., Xu, X. L., Fan, J. W. & Wang, J. B. (2018). Linking the benefits of ecosystem services to sustainable spatial planning of ecological conservation strategies. *Journal of Environmental Management, 222*, 385-395.

Jiang, Y., Tang, Y. & Li, H. (2022). A review of trends in the use of sewage irrigation technology from the livestock and poultry breeding industries for farmlands. *Irrigation Science*(3), 40.

Jiang, Y., Zhang, Y. & Li, H. (2023). Research Progress and Analysis on Comprehensive Utilization of Livestock and Poultry Biogas Slurry as Agricultural Resources. *Agriculture-Basel, 13*(12), 17.

Johannsen, L. L., Schmaltz, E. M., Mitrovits, O., Klik, A., Smoliner, W., Wang, S. & Strauss, P. (2022). An update of the spatial and temporal variability of rainfall erosivity (R-factor) for the main agricultural production zones of Austria. *Catena, 215*, 106305.

Johannsen, L. L., Zambon, N., Strauss, P., Dostal, T., Neumann, M., Zumr, D., . . . Klik, A. (2020). Impact of Disdrometer Types on Rainfall Erosivity Estimation. *Water, 12*(4).

Khanal, S., Anex, R. P., Anderson, C. J., Herzmann, D. E. & Jha, M. K. (2013). Implications of biofuel policy-driven land cover change for rainfall erosivity and soil erosion in the United States. *Global Change Biology Bioenergy, 5*(6), 713-722.

Li, X., Yang, J. & Zhao, C. (2014). Effect of agroforestry and time on soil and water conservation of sloping red soil in southeastern China. *Journal of Soil and Water Conservation, 69*(2), 131-139.

Li, Z. & Guo, X. (2018). Non-photosynthetic vegetation biomass estimation in semiarid Canadian mixed grasslands using ground hyperspectral data, Landsat 8 OLI, and Sentinel-2 images. *International journal of remote sensing, 39*(19-20), 6893-6913.

Liu, B. (2023). *Livestock carrying state estimation product in Qinghai-Tibet Plateau (2000-2019)*.

Liu, B. Y., Chen, Z. Y., Li, B., Wu, S. F., Feng, H., Gao, X. D. & Siddique, K. H. M. (2024). Modeling of driving factors and headcut rates of ephemeral gullies in the loess plateau of China using high-resolution remote sensing images. *International Journal of Digital Earth, 17*(1).

Liu, Y. H., Gao, G., Li, H. M., Liu, L. L., Fan, Z. & Wen, T. T. (2022). Spatiotemporal Variations and Causes of Wind/Rainfall Erosion Climatic Erosivity in Qinghai Province, China. *Atmosphere, 13*(10).

Lobo, G. P. & Bonilla, C. A. (2018). A simple model for estimating changes in rainfall erosivity caused by variations in rainfall patterns. *Environmental Research, 167*, 515-523.

Lu, S. J., Chen, Y. L., Duan, X. W. & Yin, S. Q. (2023). Rainfall erosivity estimation models for the Tibetan Plateau. *Catena, 229*.

Luciano, R. V., Bertol, I., Barbosa, F. T., Vázquez, E. V. & Fabian, E. L. (2009). WATER AND SOIL LOSSES THROUGH WATER EROSION UNDER OAT AND VETCH SOWN IN TWO DIRECTIONS. *Revista Brasileira De Ciencia Do Solo, 33*(3), 669-676.

Niu, H., Yao, Y. & Ren, H. (2024). *Dataset of non-photosynthetic vegetation cover on the Qinghai-Tibet Plateau grassland (2000-2020)*.

Panagos, P., Ballabio, C., Borrelli, P., Meusburger, K., Klik, A., Rousseva, S. & Alewell, C. (2015). Rainfall erosivity in Europe. *Science of the Total Environment, 511*, 801-814.

Panagos, P., Christos, K., Cristiano, B. & Ioannis, G. (2014). Seasonal monitoring of soil erosion at regional scale: An application of the G2 model in Crete focusing on agricultural land uses. *International Journal of Applied Earth Observation and Geoinformation, 27*, 147-155.

Petek, M., Mikos, M. & Bezak, N. (2018). Rainfall erosivity in Slovenia: Sensitivity estimation and trend detection. *Environmental Research, 167*, 528-535.

Shaolang, H., Fengying, L. & Xiaowu, H. (2018). Research progress of rainfall erosivity for water erosion prediction. *Bulletin of Soil and Water Conservation, 38*(2), 262-270.

Shen, D., Guo, X. & Ma, S. (2024). Study on the Coupled and Coordinated Development of Climate Investment and Financing and Green Finance of China. *Sustainability, 16*(24), 11008.

Souza, T., Gonçalves, E. P., Pereira, D. S., dos Santos, L. M., Machado, L. S. & de Souza, E. R. (2018). REDUCING EROSION IN SORGHUM CROPS WITH MULCHING. *Revista Caatinga, 31*(3), 730-736.

Vîrghileanu, M., Savulescu, I., Mihai, B. A., Bizdadea, C. G. & Paraschiv, M. G. (2024). RUSLE-based scenarios for sustainable soil management: Case studies from Romanian Subcarpathians. *European Journal of Soil Science, 75*(4).

Vrieling, A., Hoedjes, J. C. B. & van der Velde, M. (2014). Towards large-scale monitoring of soil erosion in Africa: Accounting for the dynamics of rainfall erosivity. *Global and Planetary Change, 115*, 33-43.

Wenbo, Z. (2022). *A dataset of rainfall erosivity in the Qinghai-Tibet Plateau (1960-2019)*.

Yan, Y., Jiang, Y. Y., Guo, M. M., Zhang, X. Y., Chen, Y. & Xu, J. Z. (2023). Effects of grain-forage crop type and natural rainfall regime on sloped runoff and soil erosion in the Mollisols region of Northeast China. *Catena, 222*.

Yin, Z., Feng, Q., Wang, L., Chen, Z., Chang, Y. & Zhu, R. (2022). Vegetation coverage change and its influencing factors across the northwest region of China during 2000-2019. *Journal of Desert Research, 42*(4), 11.

Yuan, L., Yue, K. Q., Gu, Z. K., Chen, H. & Chi, Y. K. (2021). Analysis of Rainfall Factors and Soil Erosion in Different Soil and Water Conservation Measures in the Karst Plateau-Mountain. *Polish Journal of Environmental Studies, 30*(6), 5343-5349.

Zeng, H., Abedin, M. Z., Lucey, B. & Ma, S. (2025). Tail risk contagion and multiscale spillovers in the green finance index and large US technology stocks. *International Review of Financial Analysis, 97*.

Zeng, W. Y., Ding, X. T., Sun, W. Y. & Mu, X. M. (2023). Improvement of satellite-based rainfall product CHIRPS in estimating rainfall erosivity on the Loess Plateau. *Land Degradation & Development, 34*(15), 4517-4528.